Report UM22-1808

$^{40}Ar/^{39}Ar$ step-heating analysis of basalt groundmass and phlogopite from Curnamona Province, SE Australia

H. Dalton and D. Phillips

School of Geography, Earth and Atmospheric Sciences
The University of Melbourne
Parkville, VIC, 3010.

August 2022

This project was enabled by NCRIS via AuScope

1. Introduction

In 2021, Chris Folkes (Geological Survey of New South Wales) supplied six basalt whole-rock samples for groundmass separation and subsequent $^{40}Ar/^{39}Ar$ step-heating analysis.

2. Methods

Supplied samples were crushed, and groundmass separated following methods described in Matchan and Phillips (2014). Separated groundmass grains were ultrasonically cleaned with 5% HNO_3 (10 minutes), 2% HF (1 minute), demineralised water (10 minutes) and finally, were rinsed in acetone. Cleaned grains were weighed and wrapped in aluminium foil envelopes, and placed into quartz glass vials together with interspersed aliquots of the flux monitor Fish Canyon Tuff sanidine (Age = 21.176 ± 0.005 Ma; Phillips et al., 2022). The package (UM#96) was then encapsulated in an outer sealed glass vial and irradiated in the CLICIT facility of the Oregon State University TRIGA Reactor for 50 MWh.

Following irradiation and cooling, $^{40}Ar/^{39}Ar$ analyses were undertaken in the Noble Gas laboratory at the University of Melbourne. Step-heating analyses were conducted on single biotite grains placed into the sample chamber of a gas-handling system equipped with a Photon Machines Fusions 10.6 CO_2 laser and connected to a Thermo Fisher Scientific ARGUSVI mass spectrometer at the University of Melbourne. Apparatus details are given in Phillips and Matchan (2013) with updated Faraday detectors now equipped with 1 x 10^{13} Ω resistors as described in Heath et al. (2018). Analytical methods follow those described by Matchan and Phillips (2014) and Heath et al. (2018). For groundmass step-heating analysis, weighed aliquots (~3-30 mg) were incrementally heated using a 6 mm laser beam-size was utilised with laser power varied (2.5–30%), dependent on number of heating steps (1-25) for each aliquot (see Appendix Table 1). All results are corrected for system blanks, mass discrimination, radioactive decay and reactor-induced interference reactions. Correction factors vary for each irradiation can and are supplied in Appendix Table A1. Mass discrimination was monitored by analysis of standard air volumes, assuming the air argon isotopic composition of Lee et al. (2006).

Analytical results are summarised below, with the full dataset provided in the Appendix (Tables 1 and A1). Inclusion of uncertainties in the J-value and age of Fish Canyon Tuff sanidine have a negligible impact on uncertainties. Decay constants are those of Steiger and Jäger (1977). The $^{40}Ar/^{39}Ar$ dating technique is described in detail by McDougall and Harrison

(1999). Age spectra were generated using ISOPLOT (Ludwig, 2003). Age uncertainties reported in the results section are 2σ unless otherwise stated.

3. Results

The step-heating spectra for the aliquots from six basalt groundmass samples are summarised in Figure 1 below. The ^{39}Ar release spectra are quite variable, ranging from near-flat to more extreme ‘hump’, ‘saddle’ and ascending ‘staircase’-shaped with apparent ages ranging from ~450 to ~1800 Ma (**Fig. 1**).

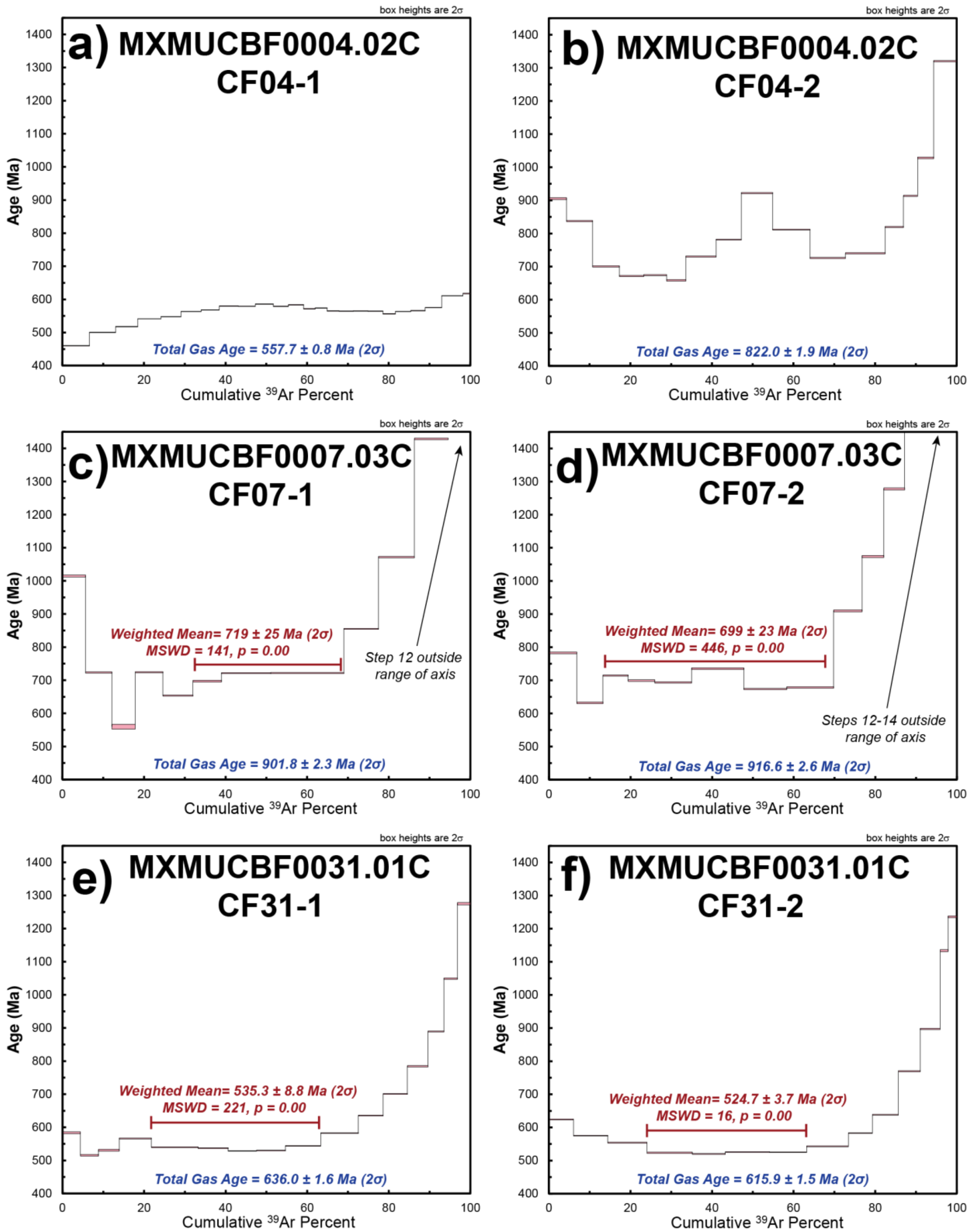

Figure 1 (*continued overleaf*): ^{40}Ar/^{39}Ar age spectra for aliquots from basalt groundmass samples. Note that all spectra have been plotted to the same scale for ease of comparison and as a result the oldest apparent ages are beyond the scale in some panels (c, d, h, j).

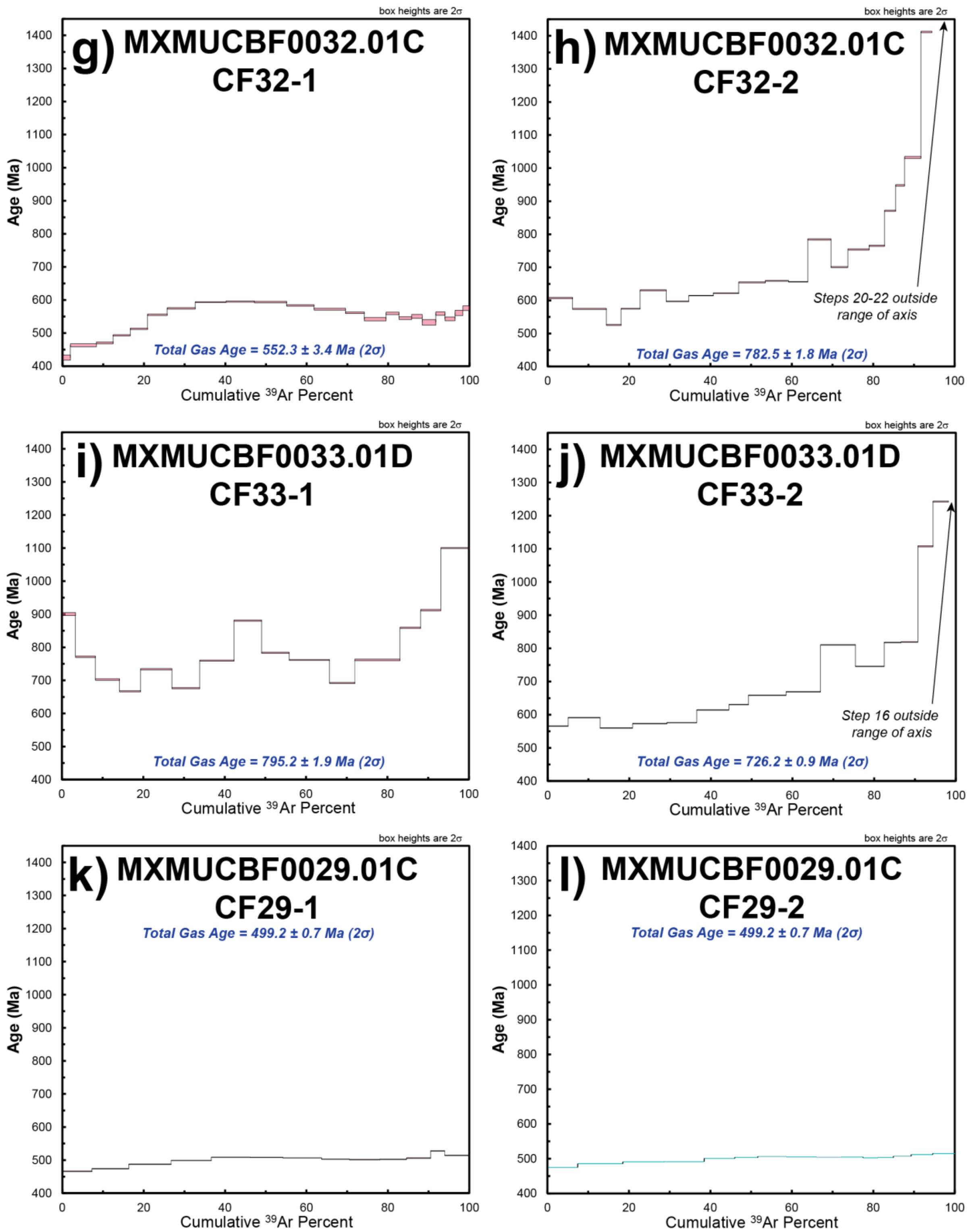

3.1 Mundi Mundi Plain: CF04 (MXMUCBF0004.02C)

The two aliquots analysed from sample CF04 yielded strongly contrasting ^{39}Ar release spectra. Aliquot CF04-1 (**Fig. 1a**) produced a spectrum with gradually increasing apparent ages which 'flattened' to ages around ~550 to 600 Ma. In contrast, the second aliquot (CF04-

2; **Fig. 1b**) produced a step-heating spectrum with alternating decreasing and increasing apparent ages where minimum apparent ages approached ~680 Ma and maximum apparent ages exceeded 1300 Ma. It should be noted that extraction of geologically meaningful age information from samples with discordant age spectra is challenging, and care must be taken to avoid over-interpretation of such data. It is possible that ^{39}Ar recoil loss/redistribution might explain the discordance observed in these aliquots, and indeed those discussed further below (e.g., Jourdan and Renne, 2014). See Hall (2014) for a thorough discussion of recoil effects on ^{40}Ar/^{39}Ar ages. In addition, it has been noted that some samples have been subject to epidote-chlorite alteration which can also contribute to the age discordance observed in the samples in this report.

However, it has been shown for both basalts and other igneous lithologies that total gas ages (an aggregate age for all heating steps weighted by the proportion of ^{39}Ar released in each step) can be within uncertainty of 'true' emplacement ages for recoil impacted samples (Dalton et al., 2020; Heath et al., 2018). To a first approximation, it appears that the step heating profile of aliquot CF04-1 is the least 'disturbed' of the two analysed for CF04 and therefore the total gas age of 557.7 ± 0.8 Ma may serve as a meaningful age estimate for this sample.

3.2 Mundi Mundi Plain: CF07 (MXMUCBF0007.03C)

Unlike the two aliquots from CF04, CF07-1 and CF07-2 produced near-identical heating spectra (**Fig. 1c,d**) with flat portions in the intermediate heating steps at apparent ages around ~700 Ma, before a later increase in apparent ages in the highest temperature steps (approaching 1800 Ma). The older apparent ages in higher temperature steps may be related to outgassing of xenocrystic material that can contain inherited argon (e.g., De Beni et al., 2005) or the impacts of recoil and/or alteration as discussed above. Given the extreme discordance in the high temperature steps, where apparent ages increase more than 500 Ma, it may not be suitable to use the total-gas ages but instead consider only the flatter, more concordant parts of the spectrum. In these instances, weighted mean calculations exclude potentially anomalous heating steps at the beginning and/or the end of the step-heating experiment. Utilising this approach, the two aliquots yield imprecise but indistinguishable weighted mean ages of 719 ± 25 Ma (CF07-1; $n = 3$) and 699 ± 23 Ma (CF07-2; $n = 6$). On this evidence, the combined weighted mean age of 708 ± 17 Ma may be the most appropriate estimate for the time of isotopic closure (e.g., *crystallisation or resetting event*) for this sample.

3.3 Wilangee Basalt: CF31 (MXMUCBF0031.01C)

The aliquots from sample CF31 produced near-identical step heating spectra, with relatively consistent apparent ages in the early to intermediate heating steps (~520-560 Ma) which increase dramatically in the latter, higher temperature steps to ages exceeding 1200 Ma (**Fig. 1e,f**). This pattern is not dissimilar to that observed for CF07, described above, although the absolute values of the apparent ages 100s of Myr. The reasons for the age discordance in CF31 may be similar to that described above for CF07, however, it is also noted that the Wilangee Basalt samples are vesicular. The presence of glass, particularly altered/devitrified glass has been shown to contribute to, sometime significant, discordance in $^{40}Ar/^{39}Ar$ step heating analysis of basaltic groundmass (e.g., Cerling et al., 1985; Fleck et al., 1977; Koppers et al., 2000; Walker and McDougall, 1982). The same is true for any alteration present for other groundmass phases (Baksi et al., 2007; Koppers et al., 2003).

When considering the 'flattest' part of the spectrum for aliquots CF31-1 and CF32-2 two indistinguishable weighted mean ages of 535.3 ± 8.8 Ma and 524.7 ± 3.7 Ma, respectively. Combining these ages returns an imprecise weighted mean age of 526 ± 48 Ma.

3.4 Wilangee Basalt: CF32 (MXMUCBF0032.01C)

The two aliquots from sample CF32 yielded contrasting ^{39}Ar release spectra, analogous to those observed for CF04. The spectrum for aliquot CF32-1 displays increasing apparent ages which plateau at ~550 to 600 Ma (again, similar to CF04-1; **Fig. 1g**), whereas CF32-2 has a much more disturbed spectrum where a progressive increase in apparent ages (>1700 Ma) is the hallmark (**Fig. 1h**). The early heating steps (steps 1-11) for the latter aliquot, have apparent ages which range between ~520 and 650 Ma. These apparent ages only slightly older than those observed for the flattest parts of the step heating spectra for aliquot CF31 described above. Considering the flattest part of the spectrum for CF32-1 (~550 to 600 Ma) and steps 1-11 for CF32-2 (~520 and 650 Ma) the 'true' emplacement age for this sample may lie somewhere between 550 and 650 Ma. Given that the spectrum for CF32-1 is much more concordant than CF32-2 it is likely that the age lies much closer to ~550 to 600 Ma.

3.5 Wilangee Basalt: CF33 (MXMUCBF0033.01D)

The step heating spectra from the two aliquots of sample CF33 are similarly disturbed but have somewhat contrasting shapes (**Fig. 1i,j)**. The spectrum from CF33-1 is typified by alternating rising (up to ~1100 Ma) and falling (as low as ~670 Ma) apparent ages, in a shape similar to CF04-1 (Mundi Mundi Plain). In contrast, the ^{39}Ar pattern from CF33-2 is one of a steady rise in apparent ages from ~565 to ~820 Ma before a dramatic increase in the final three heating steps (~1100 to 1650 Ma). It is difficult to extract meaningful age information from these spectra, however, the fatter portions of CF33-1 (~550 to 600 Ma) may provide more appropriate estimates of the actual emplacement age.

3.6 Picnic Basalt: CF29 (MXMUCBF0029.01C)

Both aliquots for sample CF29 produced near identical ^{39}Ar release spectra with apparent ages gradually increasing to around ~500 Ma before a final increase in the latter 3-4 steps up to ~515-530 Ma (**Fig. 1k,l**). The total gas ages from each aliquot are also identical at 499.2 ± 0.7 Ma, and therefore this can be considered as the best age estimate for this sample.

References

Baksi, A.K., Foulger, G.R., Jurdy, D.M., 2007. A quantitative tool for detecting alteration in undisturbed rocks and minerals—I: Water, chemical weathering, and atmospheric argon, Plates, Plumes and Planetary Processes. Geological Society of America, p. 0.

Cerling, T.E., Brown, F.H., Bowman, J.R., 1985. Low-temperature alteration of volcanic glass: Hydration, Na, K, 18O and Ar mobility. Chemical Geology: Isotope Geoscience section 52, 281-293.

Dalton, H., Giuliani, A., Phillips, D., Hergt, J., maas, R., Matchan, E.L., Woodhead, J., O'Brien, H., 2020. A comparison of geochronological methods commonly applied to kimberlites and related rocks: three case studies from Finland. Chemical Geology 558.

De Beni, E., Wijbrans, J.R., Branca, S., Coltelli, M., Groppelli, G., 2005. New results of 40Ar/39Ar dating constrain the timing of transition from fissure-type to central volcanism at Mount Etna (Italy). Terra Nova 17, 292-298.

Fleck, R.J., Sutter, J.F., Elliot, D.H., 1977. Interpretation of discordant 40Ar/39Ar age-spectra of mesozoic tholeiites from antarctica. Geochimica et Cosmochimica Acta 41, 15-32.

Hall, C.M., 2014. Direct measurement of recoil effects on 40Ar/39Ar standards. Geological Society, London, Special Publications 378, 53-62.

Heath, M., Phillips, D., Matchan, E.L., 2018. An evidence-based approach to accurate interpretation of 40Ar/39Ar ages from basaltic rocks. Earth and Planetary Science Letters 498, 65-76.

Jourdan, F., Renne, P., 2014. Neutron-induced 37Ar recoil ejection in Ca-rich minerals and implications for 40Ar/39Ar dating. Geological Society, London, Special Publications 378, 33-52.

Koppers, A.A.P., Staudigel, H., Duncan, R.A., 2003. High-resolution 40Ar/39Ar dating of the oldest oceanic basement basalts in the western Pacific basin. 4.
Koppers, A.A.P., Staudigel, H., Wijbrans, J.R., 2000. Dating crystalline groundmass separates of altered Cretaceous seamount basalts by the 40Ar/39Ar incremental heating technique. Chemical Geology 166, 139-158.
Lee, J.-Y., Marti, K., Severinghaus, J.P., Kawamura, K., Yoo, H.-S., Lee, J.B., Kim, J.S., 2006. A redetermination of the isotopic abundances of atmospheric Ar. Geochimica et Cosmochimica Acta 70, 4507-4512.
Ludwig, K.R., 2003. Isoplot 3.00: A geochronological toolkit for Microsoft Excel. Berkeley Geochronology Center Special Publication 4, 70.
Matchan, E.L., Phillips, D., 2014. High precision multi-collector 40Ar/39Ar dating of young basalts: Mount Rouse volcano (SE Australia) revisited. Quaternary Geochronology 22, 57-64.
McDougall, I., Harrison, T.M., 1999. Geochronology and thermochronology by the 40Ar/39Ar method, 2nd ed. New York : Oxford University Press.
Phillips, D., Matchan, E.L., 2013. Ultra-high precision 40Ar/39Ar ages for Fish Canyon Tuff and Alder Creek Rhyolite sanidine: New dating standards required? Geochimica et Cosmochimica Acta 121, 229-239.
Phillips, D., Matchan, E.L., Dalton, H., Kuiper, K.F., 2022. Revised astronomically calibrated 40Ar/39Ar ages for the Fish Canyon Tuff sanidine – Closing the interlaboratory gap. Chemical Geology 597, 120815.
Steiger, R.H., Jäger, E., 1977. Subcommission on geochronology: convention on the use of decay constants in geo-and cosmochronology. Earth and Planetary Science Letters 36, 359-362.
Walker, D.A., McDougall, I., 1982. 40Ar39Ar and K□Ar dating of altered glassy volcanic rocks: the Dabi Volcanics, P.N.G. Geochimica et Cosmochimica Acta 46, 2181-2190.